Metal Ion Reactivity with 1,4-Benzenedimethanethiol Monolayers on Gold

M. Venkataramanan,† K. V. G. K. Murty,† T. Pradeep,*,† W. Deepali,‡ and K. Vijayamohanan*,‡

Department of Chemistry and Regional Sophisticated Instrumentation Centre, Indian Institute of Technology, Madras 600 036, India, and Physical and Materials Chemistry Division, National Chemical Laboratory, Pune 411 008, India

Received July 2, 1999. In Final Form: July 13, 2000

Exposure of Cu^{2+} ions to 1,4-benzenedimethanethiol (BDMT) monolayers on Au in solution results in the formation of copper functionalized monolayers which have been investigated in detail by surface-enhanced Raman spectroscopy (SERS), X-ray photoelectron spectroscopy (XPS), and cyclic voltammetry (CV). Upon exposure to copper ions, the free thiol groups at the surface of the monolayer disappear indicating the replacement of protons with copper ions. The reaction leads to a red shift in the C−S stretching frequency, but most of the other features are unaffected. Relative intensities of the peaks are largely the same; however, some new features are observed suggesting minor changes in the adsorbate structure that makes additional modes observable. Thermal stability of the monolayers has been reduced substantially as a result of reaction with metal ions, indicating that the chemical binding at the Au−monolayer interface is affected. XPS shows that copper is present at the surface. Electrochemical behavior before and after Cu^{2+} ion adsorption is significantly different, and the adsorbed metal ions undergo reversible redox transformations. The cyclic voltammograms of the adsorbed copper ions are discussed in relation to the oxidation state changes in aqueous electrolyte solutions.

Introduction

Self-assembled monolayers (SAMs)[1] have been of immense interest to scientists over the past decade. These organized, well-packed, and crystalline-like assemblies impart desired chemical and physical properties to surfaces which have led to a wide variety of applications.[2] Among the various self-assembled systems, organic thiols on gold have been studied widely.[3] In addition to thiols, organic disulfides and diselenides also form SAMs on Au surfaces.[4] Surface spectroscopic and microscopic techniques such as X-ray photoelectron spectroscopy (XPS),[5] atomic force microscopy (AFM),[6] scanning tunneling microscopy (STM),[7] and surface-enhanced Raman spectroscopy (SERS)[8] have been used in characterizing these monolayers. Other techniques such as ellipsometry[3a] and electrochemical methods[9] have also been used in characterizing their structure and properties. Apart from long-chain thiols, some aromatic thiols also have been shown recently to form close-packed and stable monolayers on gold surfaces.[10] Since the monolayer surfaces have unique chemical and physical properties, chemical reactivity and surface modification studies can be carried out to modulate some of them.

Reactivity of monolayers with metals deposited by thermal evaporation has been studied earlier.[11] Interfacial structure at metal/organic interfaces under controlled

* Corresponding authors. E-mail: pradeep@acer.iitm.ernet.in; viji@ems.ncl.res.in.

† Indian Institute of Technology.

‡ National Chemical Laboratory.

(1) (a) Ulman. *An Introduction to Ultrathin Organic Films from Langmuir−Blodgett to Self-Assembly*; Academic Press: New York, 1991. (b) Ulman, A. *Chem. Rev.* **1996**, *96*, 1533.

(2) (a) Wink, Th.; Zuilen, S. J. V.; Bult, A.; Bennekom, W. P. V. *Analyst* **1997**, *122*, 43R. (b) Li, D.; Ratner, M. A.; Marks, T. J.; Zhang, C. H.; Yang, J.; Wong, G. K. *J. Am. Chem. Soc.* **1990**, *112*, 7389. (c) Hickman, J. J.; Ofer, D.; Laibinis, P. E.; Whitesides, G. M. *Science* **1991**, *252*, 688. (d) Mirkin, C. A.; Ratner, M. A. *Annu. Rev. Phys. Chem.* **1992**, *43*, 719.

(3) (a) Nuzzo, R. G.; Zegarski, B. R.; Dubois, L. H. *J. Am. Chem. Soc.* **1987**, *109*, 733. (b) Nuzzo, R. G.; Fusco, F. A.; Allara, D. L. *J. Am. Chem. Soc.* **1987**, *109*, 2358. (c) Porter, M. D.; Bright, T. B.; Allara, D. L.; Chidsey, C. E. D. *J. Am. Chem. Soc.* **1987**, *109*, 3559. (d) Bain, C. D.; Troughton, E. B.; Tao, Y.-T.; Evall, J.; Whitesides, G. M.; Nuzzo, R. G. *J. Am. Chem. Soc.* **1989**, *111*, 321. (e) Evans, S. D.; Ulman, A. *Chem. Phys. Lett.* **1990**, *170*, 462. (f) Laibinis, P. E.; Nuzzo, R. G.; Whitesides, G. M. *J. Phys. Chem.* **1992**, *96*, 5097. (g) Dubois, L. H., Zegarski, B. R.; Nuzzo, R. G. *J. Chem. Phys.* **1993**, *98*, 678.

(4) (a) Bandyopadhyay, K.; Sastry, M.; Paul, V.; Vijayamohanan, K. *Langmuir* **1997**, *13*, 866. (b) Venkataramanan, M.; Skanth, G.; Bandyopadhyay, K.; Vijayamohanan, K.; Pradeep, T. *J. Colloid Interface Sci.* **1999**, *212*, 553. (c) Bandyopadhyay, K.; Vijayamohanan, K.; Venkataramanan, M.; Pradeep, T. *Langmuir* **1999**, *15*, 5314.

(5) (a) Bain, C. D.; Evall, J.; Whitesides, G. M. *J. Am. Chem. Soc.* **1989**, *111*, 7155. (b) Pale-Grosdemange, C.; Simon, E. S.; Prime, K. L.; Whitesides, G. M. *J. Am. Chem. Soc.* **1991**, *113*, 12. (c) Bindu, V.; Pradeep, T. *Vacuum* **1998**, *49*, 63. (d) Ishida, T.; Hara, M.; Kjima, I.; Tsuneda, S.; Nishida, N.; Sasabe, H.; Knoll, W. *Langmuir* **1998**, *14*, 2092. (e) Hutt, D. A.; Leggett, G. J. *Langmuir* **1997**, *13*, 3055. (f) Bensebaa, F.; Zhou, Y.; Deslandes, Y.; Kruus, E.; Ellis, T. H. *Surf. Sci.* **1998**, *405*, L472.

(6) (a) Alves, C. A.; Smith, E. L.; Porter, M. D. *J. Am. Chem. Soc.* **1992**, *114*, 1222. (b) Liu, G.-Y.; Fenter, P.; Chidsey, C. E. D.; Oglefree, D. F.; Eisenberger, P.; Salmeron, M. *J. Chem. Phys.* **1994**, *101*, 4301. (c) Wolf, H.; Ringsdorf, H.; Delamarche, E.; Takami, T.; Kang, H.; Michel, B. M.; Gerber, C.; Jaschke, M.; Butt, H.-J.; Bamberg, E. *J. Phys. Chem.* **1995**, *99*, 7102. (d) Giancarlo, C. L.; Flynn, W. G. *Annu. Rev. Phys. Chem.* **1998**, *49*, 297.

(7) See, for example: (a) Yeo, Y. H.; McGonigal, G. C.; Yackoboski, K.; Guo, C. X.; Thomson, D. J. *J. Phys. Chem.* **1992**, *96*, 6110. (b) Camillone, N.; Eisenberger, P.; Leung, T. Y. B.; Scoles, G.; Poirier, G. E.; Tarlov, M. J. *J. Chem. Phys.* **1994**, *101*, 11031. (c) Dhirani, A.-A.; Zehner, R. W.; Hsung, R. P.; Guyot-Sionnest, P.; Sita, L. R. *J. Am. Chem. Soc.* **1996**, *118*, 3319. (d) Poirier, G. E. *Chem. Rev.* **1997**, *97*, 1117.

(8) See, for example: (a) Sobocinski, R. L.; Bryant, M. A.; Pemberton, J. E. *J. Am. Chem. Soc.* **1990**, *112*, 6177. (b) Bryant, M. A.; Pemberton, J. E. *J. Am. Chem. Soc.* **1991**, *113*, 8284. (c) Bryant, M. A.; Pemberton, J. E. *J. Am. Chem. Soc.* **1991**, *113*, 3629. (d) Chadwick, J. E.; Myles, D. C.; Garrell, R. L. *J. Am. Chem. Soc.* **1993**, *115*, 10364. (e) Bercegol, H.; Boerio, F. J. *J. Phys. Chem.* **1995**, *99*, 8763. (f) Garrell, R. L.; Chadwick, J. E.; Severance, D. L.; McDonald, N. A.; Myles, D. C. *J. Am. Chem. Soc.* **1995**, *117*, 11563. (g) Zhu, T.; Yu, H. Z.; Wang, J.; Wang, Y. Q.; Cai, S. M.; Liu, Z. F. *Chem. Phys. Lett.* **1997**, *265*, 334. (h) Schoenfisch, M. H.; Pemberton, J. E. *J. Am. Chem. Soc.* **1998**, 120, 4502. (i) Sandhyarani, N.; Skanth, G.; Berchmans, S.; Yegnaraman, V.; Pradeep, T. *J. Colloid Interface Sci.* **1999**, *209*, 154. (j) Sandhyarani, N.; Pradeep, T. *Vacuum* **1998**, *49*, 279.

10.1021/la9908642 CCC: $19.00
Published on Web 09/26/2000

conditions has been investigated by ion scattering spectroscopy (ISS) and XPS.[12] Interaction of evaporated silver on octadecanethiol monolayer on gold at 90 and 300 K was investigated by XPS, ultraviolet photoelectron spectroscopy (UPS), and ISS.[13] The conclusion of the study[13] was that at 300 K the metal deposited at the monolayer surface diffuses quickly, and resides at the monolayer−Au interface, and forms islands. The monolayer structure is not significantly affected by the metal deposition. At 90 K the evaporated metal stays at the surface, but diffuses to the interface upon warming. No evidence for evaporated metal−hydrocarbon chain interaction was found, but at the interface silver bonds with the headgroups.

Recently Ulman and co-workers[14] observed that multilayer formation arising out of the ionic interaction of Cu ions adsorbed on SAM involves interesting changes in the oxidation state. For example, they observed the +1 state in a multilayer structure when the monolayer was allowed to interact with Cu^{2+} ions in solution. Although there is some controversy in the oxidation state of Cu ions (+1 or +2) after adsorption on the SAM, recent results from XPS and voltammetry[15] confirm that Cu^{2+} ions are reduced upon adsorption to the dithiol SAM. Nevertheless, more studies are desired in this direction as the electrochemistry is reported to be complicated and irreproducible,[15] especially with respect to cycling, where irreversible destruction of organized assemblies is observed. It is also important to confirm these results with other metal ions, since the ionic interactions of various metal ions can be profitably used to make organo−inorganic superstructures.[16,17]

In our earlier study, it was shown that BDMT (1,4-benzenedimethanethiol) adsorbs on the surface of gold with the benzene ring perpendicular to the surface.[18] In this orientation, one thiol group binds to the gold as thiolate and the other thiol group is free at the surface. This free S−H group at the monolayer surface is modified by exposing it to MOBT (4-methoxybenzene thiol), which leads to the formation of a prototypical bilayer.[18]

In continuation of our earlier study[18] and following the works of Ulman et al.[14] and Bard et al.,[15] we have investigated the modification of BDMT monolayers on Au by exposing them to aqueous $CuCl_2$ solutions. This type of metal ion attachment can be of particular relevance for designing complicated multilayer structures, which have promising applications in molecular electronics. Some of the metal ion containing monolayers such as Ni(II) complexes also have interesting electrocatalytic properties.[19,20] We use XPS, SERS, and cyclic voltammetery (CV) as the characterizing tools. In addition to reactivity, we observed enhancement of the spectral intensity of some peaks in SERS. To understand the stabilities of the modified monolayers, we carried out variable-temperature surface-enhanced Raman spectroscopic (VT SERS) investigations.

Experimental Section

Monolayers were prepared on 2000 Å thick surface-enhanced Raman (SER) active gold films prepared on oxidized aluminum foils. The films show corrugations in the submicrometer scale in scanning electron microscopy and are well suited for SER spectroscopy. The methodology used for the preparation of SERS active substrates is given elsewhere.[21] Monolayers were prepared following standard literature procedure used for the preparation of alkanethiol SAMs. The gold films were exposed to 1 mM solution of the chosen thiol in absolute ethanol overnight to make the monolayer. The films were removed from the solution and washed with absolute ethanol repeatedly. After washing thoroughly, these monolayers were exposed to 1 mM solutions of $CuCl_2$ in water for 10 min. The monolayers were dried in a flow of air after rinsing in water.

Raman spectra were recorded with a Bruker IFS66v FT-IR spectrometer with a FT-Raman accessory. A Nd:YAG laser (1064 nm) was used as the excitation source. All the spectra presented are averages of 500 scans. Variable-temperature measurements in the range of room temperature (RT) to 448 K were performed with a home-built heater and a programmable temperature controller.

X-ray photoelectron spectroscopic measurements were done with Mg Kα radiation using an ESCALAB Mk II spectrometer. The binding energies were calibrated with respect to the Au $4f_{7/2}$ peak at 84.0 eV. The samples were introduced into the spectrometer immediately after washing in alcohol. The monolayers showed no effect of charging during the measurements. No desorption of monolayers from the surface was noticed during measurement as there was no change in the analyzer chamber vacuum. The electron flux of the X-ray gun was kept at 70 mW to keep beam-induced damage low. The spectra were acquired at the constant analyzer energy mode. Each spectrum was an average of 20 scans.

Electrochemical measurements were made at room temperature using a three-electrode cell comprised of a gold-coated glass working electrode, a large-area platinum flag counter electrode, and a saturated calomel reference electrode (SCE) as discussed in detail elsewhere.[9e] In brief, voltammetry was performed in an oxygen-free atmosphere with a scanning potentiostat Model 362-(EG&G PAR) using aqueous 1 M KCl for all cases, unless otherwise mentioned. Cyclic voltammetry was also performed with 1 mM $K_3Fe(CN)_6$ added to 1 M KCl as a redox probe and also for some cases with 1 mM $CuCl_2$ added to 1 M KCl solution. The preparation of the working electrodes comprised of bare Au-coated glass slides and the details of SAM formation on gold along with its characterization have been reported earlier.[4,9e] The double-layer capacitance of the electrode was measured from cyclic voltammograms performed from −100 to +500 mV at a scan rate of 500 mV/s. The current from positive and negative scan directions at +200 mV was summed and divided by twice the scan rate and normalized by the actual area to obtain the reported capacitance.[9e]

Results and Discussion

Surface-Enhanced Raman Spectroscopy (SERS). Surface-enhanced Raman spectroscopy is a valuable

(9) See, for example: (a) Chidsey, C. E. D.; Bertozzi, C. R.; Putvinski, T. M.; Mujsce, A. M. *J. Am. Chem. Soc.* **1990**, *112*, 4301. (b) Becka, A. M.; Miller, C. J. *J. Phys. Chem.* **1992**, *96*, 2657. (c) Finklea, H. O.; Snider, D. A.; Fedyk, J.; Sabatani, E.; Gafni, Y.; Rubinstein, I. *Langmuir* **1993**, *9*, 3660. (d) Campbell, D. J.; Herr, B. R.; Hulteen, J. C.; Van Duyne, R. P.; Mirkin, C. A. *J. Am. Chem. Soc.* **1996**, *118*, 10211. (e) Bandyopadhyay, K.; Vijayamohanan, K.; Shekhawat, G. S.; Gupta, R. P. *J. Electroanal. Chem.* **1998**, *447*, 11.

(10) (a) Kolega, R. R.; Schlenoff, J. B. *Langmuir* **1998**, *14*, 5469. (b) Bandyopadhyay, K.; Sastry, M.; Paul, V.; Vijayamohanan, K. *Langmuir* **1998**, *14*, 625.

(11) See, for example: (a) Czanderna, A. W.; King, D. E.; Spaulding, D. *J. Vac. Sci. Technol., A* **1991**, *5*, 2607. (b) Herdt, G. C.; Czanderna, A. W. *J. Vac. Sci. Technol., A* **1997**, *15*, 513.

(12) Herdt, G. C.; Czanderna, A. W. *J. Vac. Sci. Technol., A* **1994**, *12*, 2410.

(13) Tarlov, M. J. *Langmuir* **1992**, *8*, 80.

(14) (a) Evans, D. S.; Ulman, A.; Goppert-Berarducci, K. E.; Gerenser, L. J. *J. Am. Chem. Soc.* **1991**, *113*, 5866 (b) Freeman, T. L.; Evans, S. D.; Ulman, A. *Thin Solid Films* **1994**, 784.

(15) Brust, M.; Blass, P. M.; Bard, A. J. *Langmuir* **1997**, *13*, 5602.

(16) (a) Lee, H.; Kepley, L. J.; Hong, H. G.; Mallouk, T. E. *J. Am. Chem. Soc.* **1988**, *110*, 618. (b) Ansell, M. A.; Zeppenfeld, A. C.; Yoshimoto, K.; Cogan, E. B.; Page, C. J. *Chem. Mater.* **1996**, *8*, 591. (c) Bandyopadhyay, K.; Vijayamohanan, K. *Langmuir* **1998**, *14*, 6924.

(17) Li, D.; Bishop, A.; Gim, Y.; Shi, X. B.; Fitzsimmons, M. R.; Jia, Q. X. *Appl. Phys. Lett.* **1998**, *73*, 2645.

(18) Murty, K. V. G. K.; Venkataramanan, M.; Pradeep, T. *Langmuir* **1998**, *14*, 5446.

(19) Gobi, V. K.; Kitamara, F.; Takuda, K.; Ohsaka, T. *J. Phys. Chem. B* **1999**, *103*, 83.

(20) Berchmans, S.; Yegnaraman, V.; Sandhyarani, N.; Murty, K. V. G. K.; Pradeep, T. *J. Electroanal. Chem.* **1999**, *468*, 170.

(21) Sandhyarani, N.; Murty, K. V. G. K.; Pradeep, T. *J. Raman Spectrosc.* **1998**, *29*, 359.

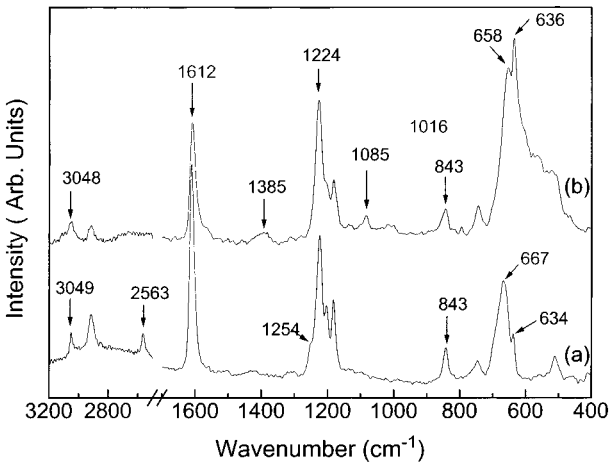

Figure 1. Surface-enhanced Raman spectra of (a) bare BDMT monolayer on Au and (b) the monolayer exposed to Cu^{2+} ions. The peaks of significance are marked (see text).

technique in characterizing SAMs on noble metal surfaces. SERS selection rules[22] are useful in predicting the orientation of the molecule on the surface. Unlike surface infrared spectroscopy, SERS enhances vibrations which are parallel as well as perpendicular to the surface, albeit to different extents. An important vibration used in the structural characterization in aromatic systems is the C−H stretching mode, which is enhanced more when the bond is perpendicular to the surface, as in the case of a benzene ring when it stands perpendicular to the surface. The major limitations are that it is applicable only to selected metals and that surface selection rules are not yet understood clearly.

Figure 1 displays the Raman spectra of the bare BDMT monolayer and that after exposure to $CuCl_2$ solution. The structure and bonding of BDMT monolayers on Au have been discussed earlier.[18] Briefly, the molecule adsorbs on the surface with one of the thiol groups in the thiolate form and the benzene ring remains perpendicular to the surface. The other thiol group projects at the surface. Temperature-dependent SERS spectra show that the monolayer is stable up to 423 K and at about 448 K it begins to desorb from the surface. The desorption occurs after a phase transition of the monolayer during which the molecule falls on the surface and both thiol groups are involved in bonding with the surface. The thiol group at the surface is a very sensitive probe for the reactivity of the monolayer. Upon exposure of the thiol functionalized surface to an alkaline solution, the S−H stretching frequency disappears completely, indicating the removal of the thiol proton.

Figure 1 shows that the peak at 2563 cm^{-1} due to S−H stretching is completely lost as a result of exposure to Cu^{2+} ions in solution. The other peaks in the region at 3054 and 2918 cm^{-1}, due to the aromatic C−H and the methylene C−H stretching modes, respectively, are unaffected as a result of metal ion exposure. The intensities of these bands seem to suggest that the monolayer geometry is unaffected. Consequent to the disappearance of the S−H mode, there are significant changes observed in the low-frequency region. An important effect is the disappearance of the methylene wagging mode at 1254 cm^{-1}. It is reasoned that as a result of the removal of the thiol proton at the surface, both methylenes become similar and the differences in the methylene modes disappear.

(22) (a) Moskovits, M. *Rev. Mod. Phys.* **1985**, *57*, 783. (b) Otta, A.; Mrozek, I.; Grabhorn, H.; Akemann, W. *J. Phys.: Condens. Matter Phys.* **1992**, *4*, 1143.

Table 1. Raman Stretching Frequencies for Solid and $CuCl_2$ Exposed BDMT Monolayers (in cm^{-1})

BDMT on Au	Cu^{2+}	assignment
510	507	
634	636	ν(C−S)
667	658	ν(C−S)
745	740	δ(C−S)
843	843	ν(C−H)
	1085	ring mode
1184	1182	β_{C-H}
1203	1205(w)[a]	
1222	1225	CH_2 wagging
1254		CH_2 wagging
1608	1612	ring deformation
2563		ν(S−H)
2926	2912	ν(C−H)
3055	3049	ν[C−H(aromatic)]

[a] w = weak.

Our earlier study[18] has also shown that the thiol hydrogen can be replaced by introducing the BDMT monolayer into a solution of another thiol where, again, the methylene wagging mode disappears. The C−S stretching modes appearing at 667 and 634 cm^{-1} in the bare BDMT monolayer are present at 658 and 636 cm^{-1} in the modified monolayer; we attribute this to the two distinct binding environments. The former one is due to the C−S attached to Cu and the other one is due to the C−S attached to Au. Note that the former undergoes a red shift upon reaction, whereas the latter is unaffected. These changes suggest that chemical changes have occurred to the monolayer chain, but the molecular orientation is the same as in the parent monolayer. It appears that the copper ion attachment has contributed to the enhancement of the intensity. As a result of the reaction, several other features appear in the spectrum. Additional peaks appear at 1385, 1085, and 1016 cm^{-1} for the Cu^{2+} exposed monolayer. The first one can be attributed to the methylene groups and the latter two can be assigned to the phenyl ring. The absence of any significant shift for the benzene ring mode appearing at 1608 cm^{-1} suggests that the ring lies perpendicular to the surface. The shoulder observed in the low wavenumber region of this band in the Cu^{2+} ion modified monolayers could be attributed to a minor structural change. The peak frequencies are summarized in Table 1.

Variable-Temperature SERS. To understand the stability of the Cu^{2+} modified monolayers and to study their temperature-dependent structural changes, we performed variable-temperature (VT) SERS measurements. Figure 2 shows the VT SERS spectra of BDMT monolayer exposed to $CuCl_2$ solution. To compare the intensities, the spectra were acquired under the same conditions. They are also presented in the same intensity scale except for the offset. The first observation is that all the BDMT features are observed up to 423 K. However, the intensities start decreasing even at 323 K. Particularly noticeable is the change in the intensity of the methylene wagging modes. This is in contrast to the case of bare BDMT,[18] where structural changes are not noticeable before the desorption of the monolayer. In the C−S region, substantial broadening is observed with increase in temperature.

General features of the spectra are in complete agreement with the literature reports quoted in the Introduction. The variable-temperature experiment clearly shows that the thermal stability of the monolayer is significantly affected upon exposure to $CuCl_2$ solution. It has been shown earlier that the rate of atomic diffusion through monolayers is substantial, leading to the migration of deposited Ag to the headgroup/Au interface in the case of

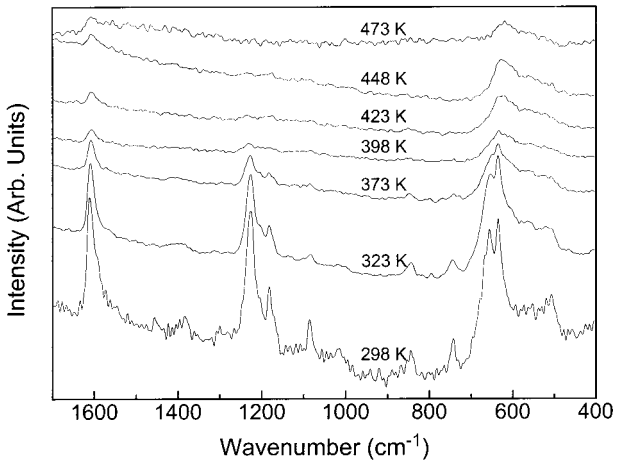

Figure 2. Surface-enhanced Raman spectra Cu^{2+} exposed to BDMT monolayers on Au as a function of temperature. The corresponding temperatures are indicated.

octadecanethiol monolayer on gold.[13,24] The migrated Ag atoms modify the headgroup−Au interaction. This diffusion is arrested only at low temperatures such as 90 K. In the case of the Cu^{2+} ion modified BDMT monolayers, it appears that as the temperature is increased the copper ions become mobile and it is likely that they reach the Au−BDMT interface and participate in bonding. This makes the Au−BDMT binding weaker, and the monolayer desorbs at a lower temperature than in the unmodified case.

X-ray Photoelectron Spectroscopy. XPS measurements reveal the presence of copper ion on the surface of the monolayer. Due to significant X-ray beam induced damage of the overlayer, no attempt has been made to deduce structural and valence state details.

Cyclic Voltammetry (CV). The effectiveness of the barrier layers formed by BDMT SAMs on gold surfaces may be assessed by examining the double layer capacitance change upon SAM formation (Figure 3A) and also by the degree of blocking of electrode reactions of redox active probes (Figure 3B). For example, an approximate estimation of the double layer capacitance on the basis of Figure 3A shows a decrease from 15.2 (bare gold) to 1.5 (BDMT covered Au) μF/cm^2, suggesting that a compact monolayer is formed. In comparison, a double layer capacitance value of 1.4 μF/cm^2 is generally obtained for well-known long-chain thiols such as octadecyl mercaptan[3c] on similar substrates, indicating the structural integrity of the BDMT SAMs. Further confirmation comes from the complete blocking of the redox behavior of a reversible couple such as $Fe(CN)_6^{3-/4-}$ as demonstrated by Figure 3B. The clear reversible, diffusion-controlled electrode process on a bare Au electrode at a formal potential ($E°'$, approximated to the midpoint of anodic and cathodic peaks) of +218 mV vs SCE is completely suppressed by the passivating nature of the BDMT monolayer on the gold electrode. The use of $Fe(CN)_6^{3-/4-}$ as a simple outer sphere redox couple for probing the integrity and uniformity of SAMs on Au electrodes is a well-established method.[3c,9e] Defective monolayers are found to give significant faradaic current, unlike that observed for the BDMT monolayer. Thus Figure 3B indicates that the contribution of the so-called "pinholes" or defects in the monolayer structure is small for the BDMT monolayer on Au in the potential range

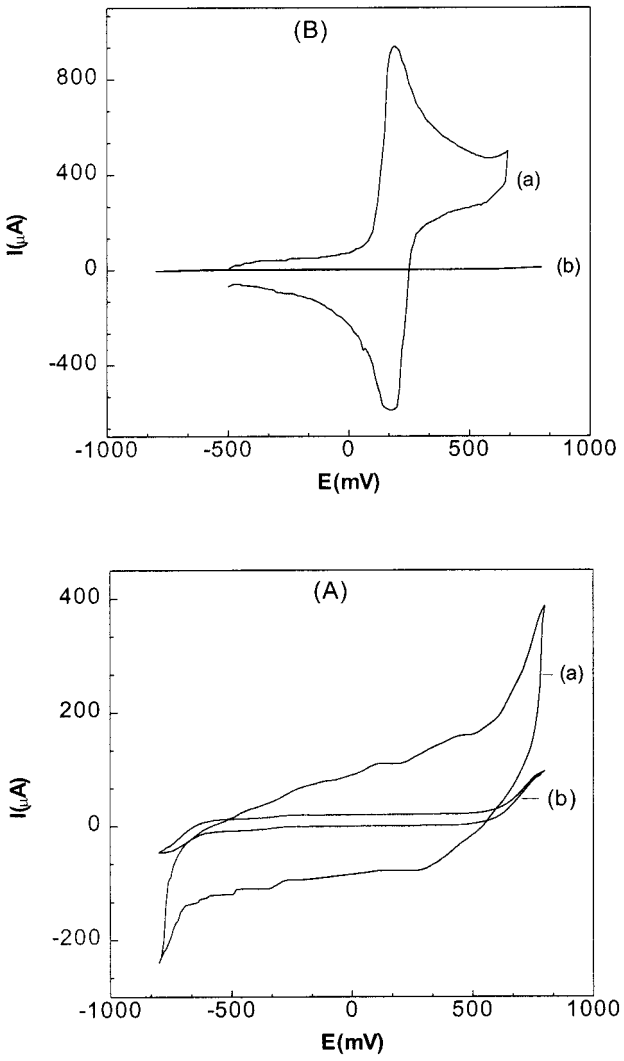

Figure 3. (A) Superimposed cyclic voltammograms of (a) bare Au electrode and (b) Au electrode covered with self-assembled BDMT monolayer in 1 M aqueous KCl solution at a scan rate of 500 mV/s. (B) Superimposed cyclic voltammograms of (a) bare Au electrode and (b) Au electrode covered with BDMT monolayer in the presence of 1 mM $K_3Fe(CN)_6$ in 1 M KCl at a scan rate of 100 mV/s.

under consideration, as the formation of the monolayer totally blocks the electron transfer.

Figure 4 shows the cyclic voltammograms of Cu(II) ions adsorbed on a SAM of BDMT on an Au electrode in 1 M aqueous KCl solution at different scan rates in the range of −200 to +600 mV vs SCE. The scan rate dependent voltammogram is important due to various reasons. First, the voltammogram corresponding to 10 mV/s is almost featureless, except for perhaps a broad region corresponding to both reversible peaks which is clearly seen for the scan rate at 20 mV/s. The well-defined reversible peaks are, however, better resolved as the scan rate increases from 50 to 100 mV/s. This can be used to calculate approximate formal potential values for the corresponding redox processes involving Cu ions. Second, the voltammetric behavior is qualitatively similar to that reported by Bard et al.,[15] for Cu ions adsorbed on a SAM of 3-mercaptopropionic acid in 0.1 M aqueous K_2SO_4. More importantly, a plot of the peak current (both anodic as well as cathodic) versus scan rate is nearly linear (see the inset of Figure 4) passing through the origin, suggesting that all adsorbed Cu ions are mostly retained on the SAM

(23) Schrader, B.; Hoffmann, A.; Keller, S. *Spectrochim. Acta* **1991**, *47A*, 1135.
(24) Oyamatsu, D.; Nishizawa, M.; Kuwabata, S.; Yoneyama, H. *Langmuir* **1998**, *14*, 3298.

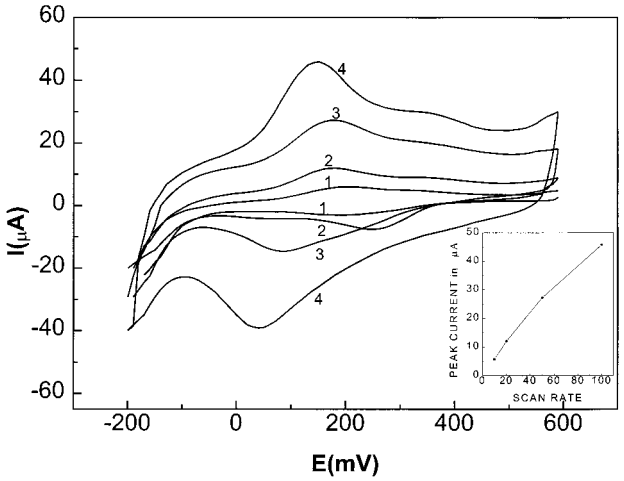

Figure 4. Cyclic voltammograms of Au electrode covered with BDMT SAM after adsorbing Cu(II) ions (from 1 mM aqueous $CuCl_2$ solution) in 1 M KCl at various scan rates; 1, 2, 3, and 4 represent scan rates of 10, 20, 50, and 100 mV/s, respectively. Inset shows the variation of peak current with scan rate to illustrate the features of surface confinement.

surface.[26] This suggestion is further supported by the diminishing separation between the anodic and cathodic peaks (ΔE_p) as the scan rate decreases. The curvature at high scan rates can be attributed to the partial destruction of the monolayer or field induced orientational changes. The shoulder on the anodic side around 400 mV (more prominent for 50 and 100 mV/s scan rates) is perhaps due to the oxidation of Cu(I) to Cu(II), confirming that Cu^{2+} ion is reduced upon adsorption on BDMT SAMs. The slopping anodic background is common for dithiol and disulfide SAMs and is often explained on the basis of slow oxidation.[16] Accessibility of all the surface-bound Cu ions for the redox transformation is suggested by an approximate calculation of the area under the peak (20 μC/cm^2) for the case of a typical voltammogram taken at 100 mV/s. For the same voltammetric response, surface concentration calculated per unit area (cm^2) of the anodic peak corresponds to 2.8×10^{-10} mol while the cathodic peak corresponds to 5.5×10^{-10} mol. The electrostatic repulsion between the bound Cu ions may be the reason for this discrepancy, as even for the case of the reduction peak observed at 50 mV/s scan rate, the reduced form is in excess. Both peak potentials are scan rate dependent, and the ratio of anodic to cathodic peak current is essentially unity. The reversible half-wave potential also corresponds to Cu(I) reduction.

The high degree of reversibility observed for the case of 100 mV/s scan rate is found to be adversely affected by repeated cycling. For example, a typical voltammogram taken under the same scan rate as represented in Figure 4 changes significantly after *four cycles* (these scans are not indicated in the figure). While the anodic peak potential shifts to 500 mV (roughly 80 mV/cycle), the cathodic peak potential becomes 150 mV (30 mV/cycle). Figure 5A shows the voltammetric data at this scan rate for five successive cycles (fifth to ninth), and the diminishing peak currents are more pronounced for the reduction case while the shift in potential with cycles is more significant for the anodic case. This may be explained on the basis of the increased electrostatic repulsion between the surface-bound Cu (linked with ligands) even in the confined state. More

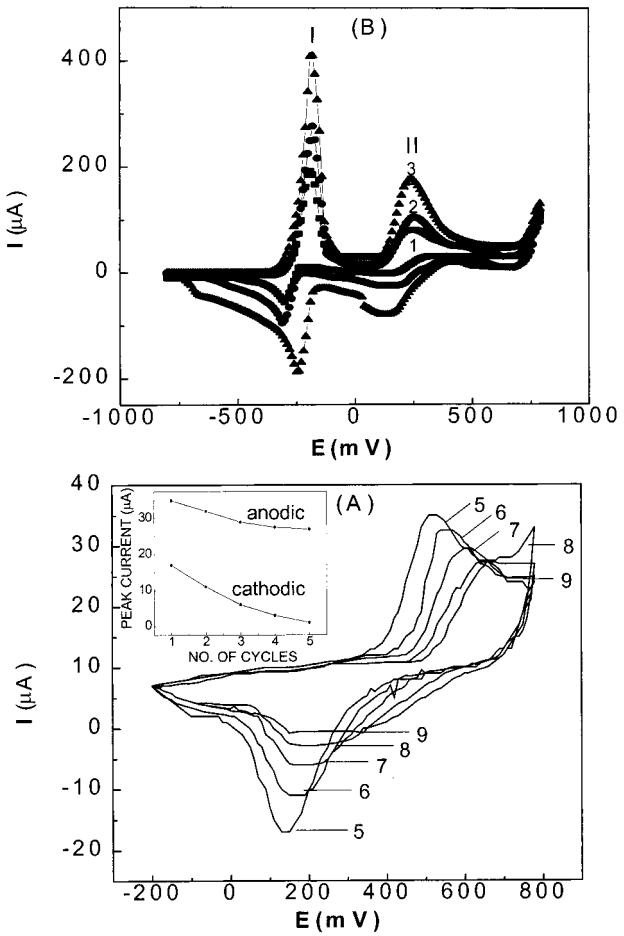

Figure 5. (A) Cyclic voltammograms of Au electrode covered with BDMT SAM after adsorbing Cu(II) ions in 1 M aqueous KCl solution at 100 mV/s scan rate (same as Figure 4) for five successive cycles starting from the fifth cycle. The variation of peak currents (for both anodic and cathodic) with number of cycles is indicated in the inset. (B) Cyclic voltammograms of Au electrode with adsorbed Cu(II) ions on BDMT SAMs (i.e., same as Figure 4) in the presence of 1 mM $CuCl_2$ added to 1 M aqueous KCl solution at (1) 20, (2) 50, and (3) 100 mV/s scan rates. I and II represent one- and two-electron reductions, respectively.

interestingly, the voltammograms obtained after five successive cycles (cf. fifth and ninth cycles in Figure 5A) show that defects are produced in the monolayer during cycling as the final shape suggests a plateau current[9c] possibly due to the presence of an array of pinholes. This is more pronounced on the anodic side as Cu(I) loss is more responsible for this, while there is a more systematic current reduction due to Cu loss (see the inset of Figure 5A). An approximate estimation of the coverage with number of cycles indicates that the loss of signal with cycles is more for the reduced form. The difference most probably results from a partial loss of bound Cu ions adversely affecting the monolayer integrity, and is revealed by the final voltammogram after eight cycles.

To learn how variation of the oxidation state of Cu ions after adsorption on the monolayer affects the redox reactions, we used a strategy of introducing Cu(II) ions directly into 1 M KCl electrolyte. The voltammogram of adsorbed Cu ions on the BDMT SAM, as indicated in Figure 5A, is found to be drastically altered when 1 mM $CuCl_2$ is added to the electrolyte. The peaks present due to the adsorbed Cu ions on the BDMT SAM are retained, but more significantly, a sharp reversible peak is formed (Figure 5B). It may be mentioned that no peak was observed in the region between −200 and −800 mV in the

(25) Briggs, D.; Seah, M. P. *Practical Surface Analysis by Auger and X-ray Photoelectron Spectroscopy*; John Wiley & Sons: New York, 1984.
(26) Brown, A. P.; Anson, F. C. *Anal. Chem.* **1977**, *49*, 1589.

absence of $CuCl_2$ in solution. The anodic peak is unusually sharp with intensity matching the reported data for underpotential deposition of Cu from Cu^{2+} ions. Similar features have been observed for the underpotential deposition of copper on SAMs of propanethiol.[27a] Since the standard potential of Cu^{2+}/Cu couple (0.3475) is less than that for Cu^{+}/Cu couple (0.522), we believe that peak I corresponds to Cu(I) reduction to Cu metal while peak II corresponds to the reduction of Cu(II) to Cu reduction. The peak width of II is also found to be double compared to peak I, confirming the involvement of two-electron and one-electron processes, respectively. These data for peak II are congruent with the occurrence of the following reaction, $Cu^{2+} + 2e \rightarrow Cu$, as a diffusion-limited process (peak current is proportional to square root of scan rate, in contrast to a linear variation for peak I) probably occurring through the pinholes in the modified SAM. Although many other interpretations could be given to the two peaks, especially due to the similarity with copper underpotential deposition on thiolate covered Au(111) surfaces (where a number of well-separated peaks are seen due to different surface sites[27b]), our studies suggest that Cu is present on the BDMT monolayer as Cu(I). At what stage the Cu(II) present in aqueous solution is converted to Cu(I) during or after adsorption is not clear, and further studies are desired to unravel the mechanism.

(27) (a) Zamborini, F. P.; Campbell, J. K.; Crooks, R. M. *Langmuir* **1998**, *14*, 640. (b) Cavalleri, O.; Kind, H.; Bittner, A. M.; Kern., K. *Langmuir* **1998**, *14*, 7292.

Conclusions

The effects of copper ion adsorption on the properties of BDMT SAMs on Au have been investigated. SERS indicates the replacement of the thiol proton on the surface of BDMT monolayer by the copper ions. This modification of the monolayer surface leads to a red shift in the C−S stretching frequencies. This region also exhibits two peaks, which may be due to the two kinds of binding metal atoms, one at each end of the molecule. Copper ion attachment at the surface of the monolayer does not lead to substantial structural changes in the monolayer. VT SERS shows that thermal stability is greatly affected for the modified monolayers. XPS shows the presence of copper at the surface of the monolayer. Electrochemical experiments confirm the presence of Cu(I) on the modified monolayer. Upon repeated cycling, the monolayer develops defects and an array of pinholes is produced. A comparison of the experimental data from SERS, XPS, and CV indicates unique features of partial reduction after adsorption of Cu(II) ions. Despite changes in the monolayer composition, the structure and integrity of the SAM are unaffected.

Acknowledgment. T.P. acknowledges financial support from the Department of Science and Technology, Government of India.

LA9908642